PHYSICAL REVIEW A, VOLUME 61, 041604(R)

Trapped atomic condensates with anisotropic interactions

S. Yi and L. You
School of Physics, Georgia Institute of Technology, Atlanta, Georgia 30332-0430
(Received 29 June 1999; published 13 March 2000)

We study ground-state properties of trapped atomic condensates with electric-field-induced dipole-dipole interactions. A rigorous method for constructing the pseudopotential in the spirit of ladder approximation is developed for general nonspherical (polarized) particles interacting anisotropically. We discuss interesting features not previously considered for currently available alkali-metal condensates. In addition, to provide a quantitative assessment for controlling atomic interactions with electric fields, our investigation may also shed a different light into the macroscopic coherence properties of the Bose-Einstein condensation (BEC) of dilute interacting atoms.

PACS number(s): 03.75.Fi, 32.80.Cy, 34.10.+x

The success of atomic Bose-Einstein condensation (BEC) [1–4] has stimulated great interest in the properties of trapped quantum gases. In standard treatments of interacting quantum gases, realistic interatomic potentials $V(\vec{R})$ are replaced by contact forms $u_0\delta(\vec{R})$ in the so-called shape-independent approximation (SIA) [5]. Such an approximation results in tremendous simplification. To date, the SIA has worked remarkably well as recent theoretical investigations [4] have successfully accounted for almost all experimental observations [6,7].

Currently available degenerate quantum gases are cold and dilute, with interactions dominated by low-energy binary collisions. When realistic interatomic potentials are assumed to be isotropic and short ranged, i.e., decreasing faster than $-1/R^3$ asymptotically for large interatomic separations R, the properties of a complete two-body collision are described by just one atomic parameter: $a_{\rm sc}$, the *s*-wave *scattering length*. The scattering amplitude is isotropic and energy independent: $f(\vec{k},\vec{k}')=-4\pi a_{\rm sc}$ for collisions involving incident momentum $\vec{k}$ scattering into $\vec{k}'$. Effective physical mechanisms exist for control of the atom scattering lengths [8–10]. If implemented, these control ''knobs'' allow for unprecedented comparison between theory and experiment over a wide range of interaction strengths. Indeed, very recently several groups have successfully implemented *Feshbach resonance* [11], thus enabling a control knob on $a_{\rm sc}$ through the changing of an external magnetic field. Other physical mechanisms also exist for modifying atom-atom interactions; e.g., the *shape resonance* due to anisotropic dipole interactions inside an external electric field [12].

Although fermions with anisotropic interactions are well studied within the context of ^{3}He fluid [13] and in *d*-wave high T_c superconductors, anisotropically interacting bosons have not been studied in great detail. In particular, we are not aware of any systematic approach for constructing an anisotropic pseudopotential [5].

In this Rapid Communication, we study the ground-state properties of trapped condensates with dipole interactions. A rigorous method is developed for constructing the anisotropic pseudopotential that can also be applied to future polar molecular BEC [14,15]. This Rapid Communication is organized as follows. First we briefly review the SIA pseudopotential approximation. We then construct an analogous effective low-energy anisotropic pseudopotential. Numerical results are then discussed for ^{87}Rb [1] inside the external E field in the JILA time-averaged orbiting potential (TOP) trap. We conclude with a brief discussion of prospects for realistic experiments.

For N trapped spinless bosonic atoms in a potential $V_t(\vec{r})$, the second quantized Hamiltonian is given by

$$\mathcal{H}=\int d\vec{r}\hat{\Psi}^\dagger(\vec{r})\left[-\frac{\hbar^2}{2M}\nabla^2+V_t(\vec{r})-\mu\right]\hat{\Psi}(\vec{r}) + \frac{1}{2}\int d\vec{r}\int d\vec{r}'\hat{\Psi}^\dagger(\vec{r})\hat{\Psi}^\dagger(\vec{r}')V(\vec{r}-\vec{r}')\hat{\Psi}(\vec{r}')\hat{\Psi}(\vec{r}), \quad (1)$$

where $\hat{\Psi}(\vec{r})$ and $\hat{\Psi}^\dagger(\vec{r})$ are atomic (bosonic) annihilation and creation fields. The chemical potential μ guarantees the atomic number $\hat{N}=\int d\vec{r}\hat{\Psi}^\dagger(\vec{r})\hat{\Psi}(\vec{r})$ conservation.

The bare potential $V(\vec{R})$ in Eq. (1) needs to be renormalized for a meaningful perturbation calculation. For bosons, the usual treatment is based on field theory and is rather involved [5,16–18]. Physically the SIA can be viewed as a valid low-energy and low-density renormalization scheme. The physics involved is rather simple: one simply replaces the bare potential $V(\vec{R})$ by the pseudopotential $u_0\delta(\vec{R})$, such that its first-order Born scattering amplitude reproduces the complete scattering amplitude $(-a_{\rm sc})$. This requires $u_0=4\pi\hbar^2 a_{\rm sc}/M$.

When an electric field is introduced along the positive z axis, an additional dipole interaction

$$V_E(\vec{R})=-u_2\frac{Y_{20}(\hat{R})}{R^3} \quad (2)$$

appears, where $u_2=4\sqrt{(\pi/5)}\alpha(0)\alpha^*(0)\mathcal{E}^2$, with $\alpha(0)$ being the polarizability and $\mathcal{E}$ the electric-field strength. As was shown in Ref. [12], this modification results in a completely new low-energy scattering amplitude

$$f(\vec{k},\vec{k}')|_{k=k'\to 0}=4\pi\sum_{lm,l'm'}t_{lm}^{l'm'}(\mathcal{E})Y_{lm}^*(\hat{k})Y_{l'm'}(\hat{k}'), \quad (3)$$

with $t_{lm}^{l'm'}(\mathcal{E})$ the reduced T-matrix elements. They are all energy independent and act as generalized scattering lengths. The anisotropic V_E causes the dependence on both incident and scattered directions, $\hat{k}$ and $\hat{k}'=\hat{R}$.

A general anisotropic pseudopotential can be constructed according to

$$V_{\rm eff}(\vec{R})=u_0\delta(\vec{R})+\sum_{l_1>0,m_1}\gamma_{l_1m_1}\frac{Y_{l_1m_1}(\hat{R})}{R^3}, \tag{4}$$

whose first Born amplitude is then given by

$$f_{\rm Born}(\vec{k},\vec{k}')=-(4\pi)^2a_{\rm sc}Y_{00}^*(\hat{k})Y_{00}(\hat{k}')$$
$$-\frac{M}{4\pi\hbar^2}\sum_{l_1m_1}\gamma_{l_1m_1}(4\pi)^2$$
$$\times\sum_{lm}\sum_{l'm'}\mathcal{T}_{lm}^{l'm'}(l_1,m_1)Y_{lm}^*(\hat{k})Y_{l'm'}(\hat{k}'), \tag{5}$$

with $\mathcal{T}_{lm}^{l'm'}(l_1,m_1)=(i)^{l+l'}\mathcal{R}_l^{l'}I_{lm}^{l'm'}(l_1,m_1)$. Both

$$I_{lm}^{l'm'}(l_1m_1)=\langle Y_{l'm'}|Y_{l_1m_1}|Y_{lm}\rangle,$$

$$\mathcal{R}_l^{l'}=\int_0^\infty dR\frac{1}{R}j_l(kR)j_{l'}(k'R),$$

can be computed analytically [20]. The $1/R^3$ form in Eq. (4) assures all $\mathcal{R}_l^{l'}$ to be $k=k'$ independent (by a change of variable to $x=kR$ in the integral). Putting

$$f_{\rm Born}(\vec{k},\vec{k}')=f(\vec{k},\vec{k}'), \tag{6}$$

one can solve for the $\gamma_{l_1m_1}(\mathcal{E})$, as $t_{lm}^{l'm'}(\mathcal{E})$ are known numerically [12,19]. This reduces to the linear equations

$$-\frac{M}{4\pi\hbar^2}\sum_{l_1m_1}\gamma_{l_1m_1}(4\pi)\mathcal{T}_{lm}^{l'm'}(l_1,m_1)\equiv t_{lm}^{l'm'}, \tag{7}$$

for all (lm) and $(l'm')$ with $l,l'\neq 0$, and separately $a_{\rm sc}(\mathcal{E})=-t_{00}^{00}(\mathcal{E})$. The problem simplifies further for bosons (fermions), as only even (odd) (l,l') terms are needed to match. Figure 1 displays the result of $a_{\rm sc}(\mathcal{E})$ for the triplet state of ^{87}Rb. The Born amplitude for the dipole term V_E is

$$f_{\rm Born}(\vec{k},\vec{k}')=u_2\frac{M}{4\pi\hbar^2}(4\pi)^2\mathcal{T}_{00}^{20}\sum_{lm,l'm'}\overline{\mathcal{T}}_{lm}^{l'm'}Y_{lm}^*(\hat{k})$$
$$\times Y_{l'm'}(\hat{k}'), \tag{8}$$

with $\mathcal{T}_{00}^{20}=-0.023\,508$.

We found that, away from *shape resonances*, Table I agrees (to within approximately a few per cent) with the same ratios $t_{lm}^{l'm'}(\mathcal{E})/t_{00}^{20}(\mathcal{E})$ from the numerical multichannel calculations [12]. This interesting observation applies for all bosonic alkali-metal triplet states we computed: ^{7}Li, ^{39,41}K, and ^{85,87}Rb, for up to a field strength of 3×10^6 (V/cm) [12,19]. Physically, this implies that the effect of V_E is perturbative as $\mathcal{E}$ remains small in atomic units. What is remarkable is that $\mathcal{T}_{00}^{20}(\mathcal{E})$ and $t_{00}^{20}(\mathcal{E})$ also agree in absolute values [12]. For ^{87}Rb, we found

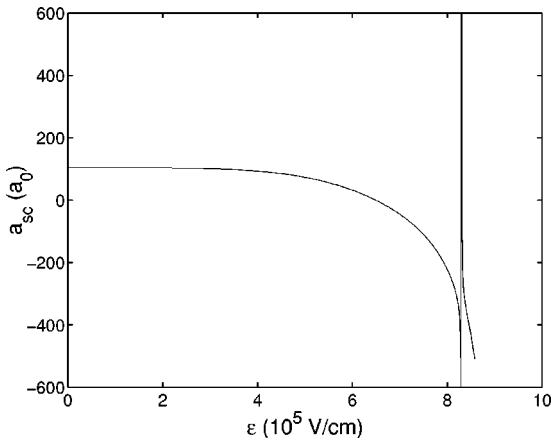

FIG. 1. The field-dependent value for $a_{\rm sc}$. Note the shape resonance for $\mathcal{E}$ around 8.3×10^5 V/cm.

$$u_2\frac{M}{4\pi\hbar^2}(4\pi)^2\mathcal{T}_{00}^{20}=-1.495\times10^{10}\overline{\mathcal{E}^2}(a_0), \tag{9}$$

with $\overline{\mathcal{E}}$ in atomic units (5.142×10^9 V/cm). a_0 is the Bohr radius, while multichannel scattering gives [19]

$$(4\pi)t_{00}^{20}=-1.512\times10^{10}\overline{\mathcal{E}^2}(a_0). \tag{10}$$

The cause of this slight difference (1%) is not entirely clear but is within numerical error.

We can thus approximate Eq. (4) by keeping only the $l_1=2,m_1=0$ term in the sum

$$V_{\rm eff}(\vec{R})=u_0\delta(\vec{R})-u_2Y_{20}(\hat{R})/R^3, \tag{11}$$

away from the *shape resonance*. At zero temperature the condensate wave function $\psi(\vec{r},t)=\langle\hat{\Psi}(\vec{r},t)\rangle$ then obeys the following nonlinear Schrödinger equation

$$i\hbar\frac{d}{dt}\psi(\vec{r},t)=\left[-\frac{\hbar^2}{2M}\nabla^2+V_t(\vec{r})-\mu+u_0|\psi(\vec{r},t)|^2\right.$$
$$\left.-u_2\int d\vec{r}'\frac{Y_{20}(\hat{R})}{R^3}|\psi(\vec{r}',t)|^2\right]\psi(\vec{r},t), \tag{12}$$

TABLE I. $\overline{\mathcal{T}}_{lm}^{l'm'}=\mathcal{T}_{lm}^{l'm'}(2,0)/\mathcal{T}_{00}^{20}$ for small (l,l').

$(lm),(l'm')$	(00)	(20)	(40)	(60)	(80)
(00)	0	1	0	0	0
(20)	1	−0.638 89	0.142 87	0	0
(40)	0	0.142 87	−0.174 20	0.056 37	0
(60)	0	0	0.056 37	−0.081 31	0.030 08
(80)	0	0	0	0.030 08	−0.047 07

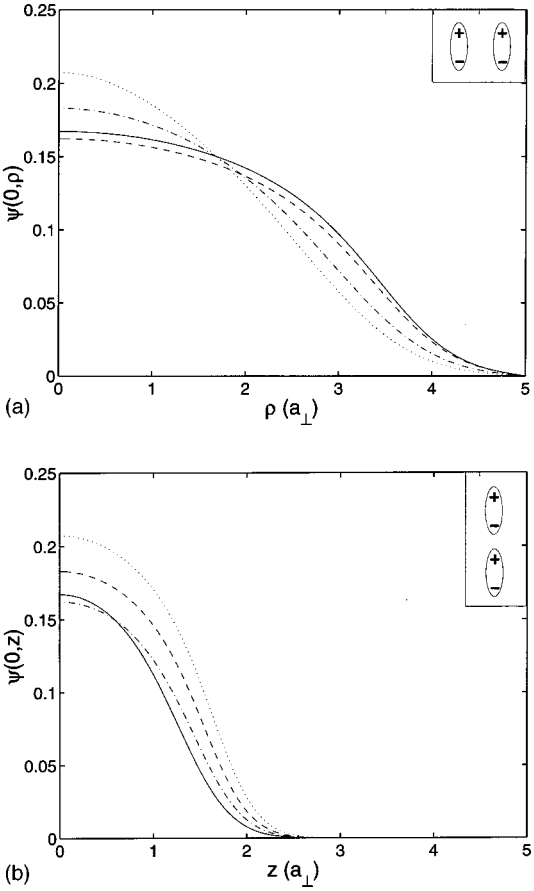

FIG. 2. (a) $\psi(\rho,0)$ for ^{87}Rb with $\omega_\perp=(2\pi)70$ Hz, $\omega_z=\sqrt{8}\omega_\perp$, and $N=5000$ atoms. Solid, dashed-dot, dashed, and dotted lines are for $\mathcal{E}=0$, 4.0×10^5, 5.7×10^5, and 5.88×10^5 V/cm, respectively. $a_\perp$ is the radial trap width. (b) Same as in Fig. 2 (a), but for $\psi(0,z)$.

with $\psi(\vec{r},t)$ normalized to N. The ground state is found by steepest descent through propagation of Eq. (12) in imaginary time (it). For a cylindrical symmetric trap $V_t(\vec{r})=M(\omega_\perp^2x^2+\omega_\perp^2y^2+\omega_z^2z^2)/2$, the ground state also possesses azimuthal symmetry. Therefore the nonlocal term simplifies to

$$\int d\vec{r}'|\psi(\rho',z')|^2\frac{Y_{20}(\hat{R})}{R^3}=\int dz'd\rho'\mathcal{K}(.,.;.)|\psi(\rho',z')|^2,$$

with the kernel $\mathcal{K}(\rho,\rho';z-z')$ expressed in terms of the standard elliptical integrals $E[.]$ and $K[.]$. The kernel is divergent at $\vec{r}=\vec{r}'$, so a cut-off radius R_c is chosen such that $\mathcal{K}(\rho',\rho,z'-z)=0$ whenever $|\vec{r}-\vec{r}'|<R_c$. We typically $R_c\sim50(a_0)$, much smaller than the grid size, to minimize numerical errors. Technical details for numerical computations and for handling the singular rapid variation of the kernel over small length scale will be discussed elsewhere [20].

Figure 2 presents $\psi(\rho,z)$ along $\rho=0$ (a) and $z=0$ (b) cuts, respectively, for ^{87}Rb ($a_{sc}=5.4$ nm) at several different $\mathcal{E}$. We note that the condensate shrinks radially while it stretches along the z axis to minimize the dipole interaction

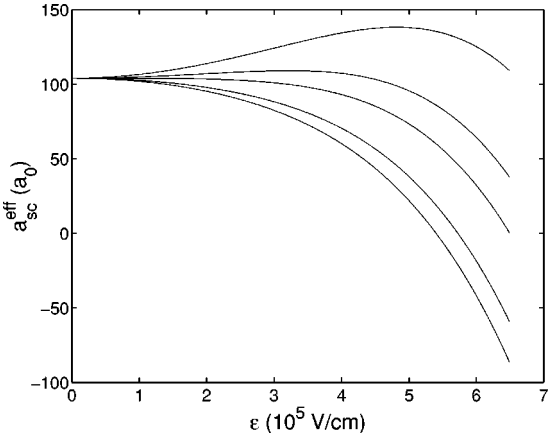

FIG. 3. Typical behavior of the effective scattering length a_{sc}^{eff}. Lines corresponds to $\kappa=5.1,1.7,1.02,0.34,0.017$, in descending order of a_{sc}^{eff}.

V_E. The top-right corner inset shows the electric-field-polarized atoms in (radially) repulsive (a) and (longitudinally) attractive (b) configurations. An elongated condensate along the z axis reduces the total energy. The same mechanism could cause spontaneous alignment of polar molecular condensates inside isotropic traps [14]. For better insights we try a variation ansatz

$$\psi_T(\rho,z)=\frac{\kappa^{1/2}}{\pi^{3/4}d^{3/2}}\exp\left[-\frac{1}{2d^2}(\rho^2+\kappa^2z^2)\right], \qquad (13)$$

with parameters d and κ. In dimensionless units for length $(a_\perp=\sqrt{\hbar/M\omega_\perp})$, energy $(\hbar\omega_\perp)$, and $\lambda=\omega_z/\omega_\perp$, we obtain

$$E[\psi_T]=\left(1+\frac{\lambda^2}{2\kappa^2}\right)d^2+\left(1+\frac{\kappa^2}{2}\right)\frac{1}{d^2}+\frac{4N\kappa}{\sqrt{2\pi}}\frac{a_{sc}^{eff}}{a_\perp}\frac{1}{d^3}, \qquad (14)$$

with the effective scattering length $a_{sc}^{eff}=a_{sc}[1-b(\kappa)u_2/u_0]$, and

$$b(\kappa)=\frac{\sqrt{5\pi}}{3(\kappa^2-1)}\left(-2\kappa^2-1+\frac{3\kappa^2\tanh^{-1}\sqrt{1-\kappa^2}}{\sqrt{1-\kappa^2}}\right).$$

The $b(\kappa)$ is monotonically decreasing, and bounded between $b(0)=\sqrt{5\pi}/3$ and $b(\infty)=-2\sqrt{5\pi}/3$. a_{sc}^{eff} is shown in Fig. 3 as a function of $\mathcal{E}$ for several different values of κ. For increasing electric field $\mathcal{E}$, variational calculation results in decreasing κ, and eventually κ becomes less than 1, i.e., the condensate changes from oblate (pancake) shaped at zero field (for the TOP trap) to prolate (cigar) shaped. We also note that $b(\kappa)\geqslant0$ for $\kappa\leqslant1$; therefore a_{sc}^{eff} becomes negative at a certain field value $\mathcal{E}_c$ in the case of a positive $a_{sc}(\mathcal{E}=0)$, causing the collapse of the condensate. This is indeed what we found as illustrated in Fig. 4. A detailed discussion of the collapse and other interesting features will be given elsewhere [21,22].

We note the energy of dipole alignment

$$E_P\sim-(2\pi)(1\times10^{18})\overline{\mathcal{E}^2}(\text{Hz}), \qquad (15)$$

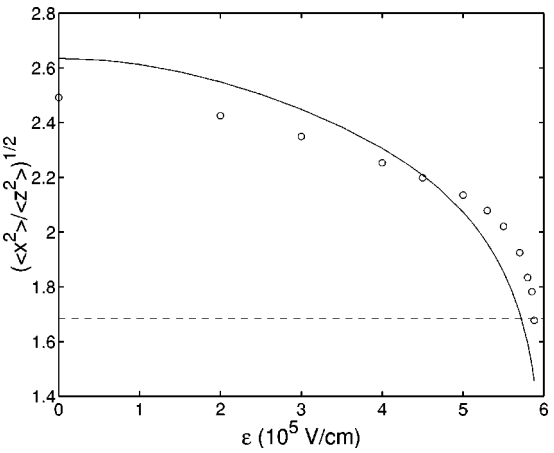

FIG. 4. Electric-field dependence of the width aspect ratio for parameters of Fig. 2. The solid line is the result of our variational calculation while circles denote exact numerical results. The dashed line corresponds to $\sqrt{\sqrt{8}}$, for a noninteracting gas in a TOP trap.

becomes much larger than the trap depth at the proposed $\mathcal{E}$ values for ^{87}Rb. Therefore spatial homogeneity for $\mathcal{E}(\vec{r})$ is required. At $\mathcal{E}\sim 5\times 10^5$ V/cm ($\bar{\mathcal{E}}\sim 10^{-4}$) with a spatial gradient $<10^{-4}/\mathrm{cm}^3$, the corresponding force is smaller than the magnetic trapping force for typical traps at ~ 100 Hz. For comparison, the magnetic-field gradient is $\sim 10^{-6}/\mathrm{cm}^3$ inside the Penning trap magnets. Although the proposed electric field (10^5 V/cm$<\mathcal{E}<10^6$ V/cm) is large, it can be created through careful laboratory techniques as breakup is fundamentally limited by field ionization, which typically occurs at $\mathcal{E}>10^7$ V/cm [23]. Recently an $\mathcal{E}$ field of up to 1.25×10^5 V/cm was used successfully to decelerate a molecular beam [24].

In conclusion, we have developed a general scheme for constructing effective pseudopotentials for anisotropic interactions. Our scheme guarantees that the first-order Born scattering amplitude from the pseudopotential reproduces the complete scattering amplitude obtained from a multichannel computation, including the anisotropic dipole interaction, thus containing no energy dependence at low temperatures of the trapped atomic gases [12]. Our scheme is thus more pleasing than the standard Skyrme-type velocity-dependent effective potentials commonly adopted in nuclear physics [25]. We also presented results for both the electric-field-modified atomic scattering parameters and the induced changes to the condensate for ^{87}Rb in the JILA TOP trap. Our theory can be directly extended to systems involving the magnetic dipole interaction of atoms/molecules in a static magnetic trap and systems of trapped molecules with permanent electric dipoles [14,26]. For alkali-metal atoms, typical magnetic dipole interaction is weak since a Bohr magneton ($\mu_B=e\hbar/2mc$) only corresponds to an electric dipole of $\sim(1/2\alpha_f)(ea_0)$ (fine-structure constant $\alpha_f\approx 1/137$), which is equivalent to the induced electric dipole at $\mathcal{E}=6\times 10^4$ V/cm for ^{87}Rb. Other atoms with larger magnetic dipole moments [27] will display clearer anisotropic effects. Typical heteronuclear diatomic molecules have a permanent electric dipole moment of $\sim(ea_0)$, corresponding to an induced moment in ^{87}Rb at $\mathcal{E}=1.6\times 10^7$ V/cm [14]. Trapped molecules with aligned permanent electric dipoles (by an external E field) would give similar results. However, magnetic trapped molecules [14], with unaligned electric dipoles interacting with the spin axis, represent an interesting extension that requires further investigation.

This work is supported by U.S. Office of Naval Research Grant No. 14-97-1-0633 and by NSF Grant No. PHY-9722410.

[1] M.H. Anderson *et al.*, Science **269**, 198 (1995).
[2] K.B. Davis *et al.*, Phys. Rev. Lett. **75**, 3969 (1995).
[3] C.C. Bradley *et al.*, Phys. Rev. Lett. **75**, 1687 (1995); **79**, 1170 (1997).
[4] An extensive list of references exists at http://amo.phy.gasou.edu/bec.html/bibliography.html.
[5] Kerson Huang and C.N. Yang, Phys. Rev. **105**, 767 (1957).
[6] M. Naraschewski and R.J. Glauber, Phys. Rev. A **59**, 4595 (1999).
[7] B. Esry and C. Greene, Phys. Rev. A **60**, 1451 (1999).
[8] P.O. Fedichev *et al.*, Phys. Rev. Lett. **77**, 2913 (1996); J.L. Bohn and P.S. Julienne, Phys. Rev. A **56**, 1486 (1997).
[9] A.J. Moerdijk *et al.*, Phys. Rev. A **53**, 4343 (1996).
[10] E. Tiesinga *et al.*, Phys. Rev. A **46**, R1167 (1992).
[11] S. Inouye *et al.*, Nature (London) **392**, 151 (1998); Ph. Courteille *et al.*, Phys. Rev. Lett. **81**, 69 (1998); J.L. Roberts *et al.*, *ibid.* **81**, 5109 (1998); Vladan Vuletic *et al.*, *ibid.* **82**, 1406 (1999).
[12] M. Marinescu and L. You, Phys. Rev. Lett. **81**, 4596 (1998).
[13] A.J. Leggett, Rev. Mod. Phys. **47**, 331 (1975).
[14] J.D. Weinstein *et al.*, Nature (London) **395**, 148 (1998).
[15] J. T. Bahns *et al.* (unpublished).
[16] V. Galitskii, Zh. Éksp. Teor. Fiz. **34**, 151 (1958) [Sov. Phys. JETP **34**, 104 (1958)].
[17] S.T. Beliaev, Zh. Éksp. Teor. Fiz. **34**, 417 (1958) [Sov. Phys. JETP **7**, 289 (1958)]; N.M. Hugenholtz and D. Pines, Phys. Rev. **116**, 489 (1959).
[18] K.A. Brueckner and K. Sawada, Phys. Rev. **106**, 1117 (1957).
[19] M. Marinescu and L. You (unpublished).
[20] S. Yi and L. You (unpublished).
[21] E.P. Gross, Nuovo Cimento **20**, 454 (1961); L. Pitaevskii, Zh. Éksp. Teor. Fiz. **40**, 646 (1961) [Sov. Phys. JETP **13**, 451 (1961)].
[22] G. Baym and C.J. Pethick, Phys. Rev. Lett. **76**, 6 (1996); Victor M. Perez-Garcia *et al.*, *ibid.* **77**, 5320 (1996).
[23] R.V. Latham, *High Voltage Vacuum Insulation: The Physical Basis* (Academic Press, New York, 1981); T.B. Mitchell, in *Non-Neutral Plasma Physics II*, edited by J. Fajans and D.H.E. Dubin, AIP Conf. Proc. 331 (AIP, Woodbury, NY, 1995), p. 115; J.C. Davis (private communications).
[24] H.L. Bethlem *et al.*, Phys. Rev. Lett. **83**, 1558 (1999).
[25] P. Ring and P. Schuck, *The Nuclear Many-Body Problem* (Springer-Verlag, New York, 1980), p. 172.
[26] K. Goral *et al.*, e-print cond-mat/9907308.
[27] J. Weinstein *et al.*, Phys. Rev. A **57**, R3173 (1998).